Homopolymerization and Block Copolymerization of N-Vinylpyrrolidone by ATRP and RAFT with Haloxanthate Inifers

ARTICLE *in* MACROMOLECULES · NOVEMBER 2009

Impact Factor: 5.8 · DOI: 10.1021/ma901578z

5 AUTHORS, INCLUDING:

Chih-Feng Huang
National Chung Hsing University
82 PUBLICATIONS **1,801** CITATIONS

SEE PROFILE

Macromolecules
ARTICLE

Macromolecules **XXXX**, *XXX*, 000–000 **A**
DOI: 10.1021/ma901578z

Homopolymerization and Block Copolymerization of *N*-Vinylpyrrolidone by ATRP and RAFT with Haloxanthate Inifers

Chih-Feng Huang,[†,‡] Renaud Nicolaÿ,[†] Yungwan Kwak,[†] Feng-Chih Chang,[‡] and Krzysztof Matyjaszewski*[,†]

[†]*Department of Chemistry, Carnegie Mellon University, 4400 Fifth Avenue, Pittsburgh, Pennsylvania 15213, and* [‡]*Department of Applied Chemistry, National Chiao Tung University, Hsinchu 30050, Taiwan*

Received July 19, 2009; Revised Manuscript Received August 12, 2009

ABSTRACT: Difunctional haloxanthate inifers were used for successive reversible addition−fragmentation transfer (RAFT) polymerization of *N*-vinylpyrrolidone (NVP) and atom transfer radical polymerization (ATRP) of styrene (St), methyl acrylate (MA), and methyl methacrylate (MMA). Since a quantitative dimerization of NVP in the presence of bromoxanthate inifers occurred, two chloroxanthate inifers, *S*-[1-methyl-4-(6-chloropropionate)ethyl acetate] *O*-ethyl dithiocarbonate (**CPX**) and *S*-[1-methyl-4-(6-chloroisobutyrate)ethyl acetate] *O*-ethyl dithiocarbonate (**CiBX**), were synthesized. These two difunctional chloroxanthate inifers were used to prepare PNVP-*b*-PSt, PNVP-*b*-PMMA, and PNVP-*b*-PMA block copolymers, where each block was synthesized by different polymerization procedures (either RAFT or ATRP). In the RAFT-first approach, well-controlled polymerization of NVP was observed. Well-defined PNVP-*b*-PSt ($M_{n,GPC}$ = 15,000 g/mol and M_w/M_n < 1.4) and PNVP-*b*-PMMA ($M_{n,GPC}$ = 50,600 g/mol and M_w/M_n < 1.3) were successfully synthesized through a subsequent chain extension by ATRP. A reshuffling reaction between propagating acrylate radicals and the xanthate moiety next to the NVP unit occurred for the preparation of PNVP-*b*-PMA, resulting in poor control of the MA chain extension. In the ATRP-first approach, a well-controlled polymerization was observed only for the ATRP of MMA with the **CiBX** initiator (M_n = 13,000 and M_w/M_n < 1.3). Significant reshuffling reactions between the xanthate moiety and styryl/acrylate propagating radicals were observed with the **CPX** initiator. This resulted in poor control and broad molecular weight distribution for the subsequent RAFT chain extension of NVP. Thus, the chloroxanthate inifers provide synthetic access to well-defined PNVP-*b*-PSt and PNVP-*b*-PMMA, but not to PNVP-*b*-PMA block copolymers.

Introduction

Recently, controlled/living radical polymerization (CRP)[1,2] has been extensively used for the polymerization of a wide range of monomers in various reaction media, showing tolerance to numerous functionalities, control over molecular weights, and narrow molecular weight distribution. Atom transfer radical polymerization (ATRP)[3−6] and degenerative transfer polymerization (DT)[7−11] are two major CRP techniques. However, the contribution of both mechanisms in one process is also possible.[12−15] CRP techniques provide an easy access to many new well-defined (co)polymers.[16−23]

In ATRP, the propagating radicals are stabilized by resonance and inductive effects and successfully polymerized monomers include styrenics, (meth)acrylates, (meth)acrylamides, and acrylonitrile.[24−27] In spite of the significant improvements in the ATRP catalytic systems,[28−30] polymerization of less reactive monomers such as vinyl acetate (VAc),[31−33] *N*-vinylpyrrolidone (NVP),[34] or *N*-vinylcarbazole (NVK)[35] still faces difficulties.

These monomers can be, however, polymerized by degenerative transfer (DT) processes such as cobalt-mediated,[36−38] alkyl iodides,[7,39] organo-stibine/tellurium/bismuthine-mediated,[10,40−42] and reversible addition−fragmentation chain transfer (RAFT)[43,44] procedures. In the RAFT procedure, the effectiveness of a chain transfer agent (CTA) for a specific polymerization clearly depends on the monomer being polymerized as well as the structures of the radical leaving group R and the stabilizing group Z.[45] Hence, RAFT agents having proper R and Z groups can be used to overcome ATRP limitations for the polymerization of nonconjugated monomers.[46]

N-Vinylpyrrolidone (NVP) is a nonconjugated monomer, and the resulting polymer (PNVP) has been widely used in numerous medical (e.g., it was used as a plasma expander during the second world war), pharmaceutical, and cosmetic applications because of its low toxicity and good biocompatibility.[47,48] Therefore, PNVP-based block copolymers can significantly expand the range of applications. However, the preparation of PNVP-based block copolymers with more reactive monomers is challenging, when using a single polymerization technique.

RAFT homopolymerization of NVP has been successfully conducted with xanthates[49] and dithiocarbamates[50] as mediating agents. PNVP block copolymers were prepared by RAFT chain extension,[50,51] transformation from ATRP to RAFT,[52] a combination of nitroxide-mediated polymerization (NMP) and RAFT,[53] anionic polymerization and NMP,[54] cobalt-mediated radical polymerization (CMRP),[55] and others.[48,56−59]

Yagci et al. and Du Prez et al. recently reviewed the syntheses of block copolymers using heterofunctional initiators containing two or more different initiation sites that are capable of initiating different polymerization mechanisms independently and selectively.[60] Such heterofunctional initiators can be efficiently applied to syntheses of block copolymers from mechanistically incompatible monomers without the need for chain end trans formation and protection steps.[61] Thus, suitable ARTP and RAFT

*To whom correspondence should be addressed. E-mail: km3b@andrew.cmu.edu.

difunctional initiators can be designed for the preparation of well-defined PNVP block copolymers.

It was recently demonstrated that ATRP and RAFT can be combined to synthesize well-defined poly(vinyl acetate) (PVAc) block copolymers using difunctional xanthate inifers.[15,62] However, this approach is more challenging for NVP since side reactions have been reported during the RAFT polymerizations of NVP with xanthates.[63] These side reactions include the formation of unsaturated and saturated dimers as well as the formation of side products in the presence of impurities such as water or acid. The xanthate moiety can also undergo elimination at higher temperatures (> 70 °C), resulting in the formation of an unsaturated chain end and a new xanthate species. Therefore, unlike VAc, RAFT polymerization of NVP encounters several potential side reactions that could have a significant influence on polymerization kinetics, end group functionality, and the resulting molar mass distributions.

The aim of the present study is to combine RAFT polymerization of NVP with ATRP of styrene and (meth)acrylates to prepare well-defined PNVP block copolymers. Several chloro- and bromoxanthate inifers were synthesized, and the order of polymerization (RAFT to ATRP or reverse) was varied in order to evaluate and optimize the block copolymer synthesis.

Experimental Section

Materials. Styrene (St, 99%), methyl methacrylate (MMA, 99%), methyl acrylate (MA, 99%), and *n*-butyl acrylate (BA, 99%) were purchased from Aldrich and purified by passing through a column filled with basic alumina to remove the inhibitors or antioxidants. *N*-Vinylpyrrolidone (NVP, 99%, Aldrich) was dried over anhydrous magnesium sulfate and purified by distillation under reduced pressure. 2,2′-Azobis(isobutyronitrile) (AIBN, 99%, Aldrich) was recrystallized twice from methanol. 2-Chloropropionyl chloride (97%), pyridine (98%), 2,2′-bipyridyne (bpy, 99%), *N*,*N*,*N*′,*N*″,*N*″-pentamethyldiethylenetriamine (PMDETA, 99%), 2,6-di(*tert*-butyl) pyridine (DtBuP, 97%), copper(II) chloride ($CuCl_2$, 99%), ethyl 2-bromopropionate (EBP, 97%), ethyl 2-bromoisobutyrate (EBiB, 98%), ethyl 2-chloropropionate (ECP, 97%), and ethyl 2-chloroisobutyrate (ECiB, 98%) were purchased from Aldrich and used without further purification. Copper(I) chloride (CuCl, 98%, Acros) was washed with glacial acetic acid in order to remove any soluble oxidized species, filtered, washed with ethanol, and dried. Tris[(2-pyridyl)methyl]amine (TPMA, 99%) was purchased from ATRP Solutions Inc. *O*-Ethyl-*S*-(1-ethoxycarbonyl)ethyl xanthate (X), *S*-(1-methyl-4- hydroxyethyl acetate) *O*-ethyl dithiocarbonate, *S*-[1-methyl-4-(6-bromoisobutyrate)ethyl acetate] *O*-ethyl dithiocarbonate (**BiBX**), and *S*-[1-methyl-4-(6-bromopropionate)ethyl acetate] *O*-ethyl dithiocarbonate (**BPX**) were prepared as described elsewhere.[15] All other solvents were purified by distillation prior to use.

General Procedure for the NVP Dimerization. In a typical experiment, EBP (12 μL, 95×10^{-3} mmol), anisole (0.25 mL), and NVP (0.5 mL, 4.69 mmol) were charged to a Schlenk flask. The resulting mixture was deoxygenated by three freeze−pump−thaw cycles. The flask was placed in an oil bath thermostatted at 60 °C. After completion of the reaction, ^{1}H NMR was used to assess the NVP dimerization. ^{1}H NMR ($CDCl_3$, δ = ppm): 6.94−6.98 (d, −CH═C*H*-N-, 1H), 4.93−4.80 (m, CH_3CHCH═CH-N-, 2H), 3.47−3.19 (m, (−N-C$H_2$$CH_2$−)×2, 4H), 2.47−2.32 (m, (−$CH_2C$$H_2$CO−) × 2, 4H), 2.12−1.90 (m, (−$CH_2C$$H_2$$CH_2$CO−) × 2, 4H).

Synthesis of *S*-[1-Methyl-4-(6-chloropropionate)Ethyl Acetate] *O*-Ethyl Dithiocarbonate (CPX). The chloroxanthate inifer, **CPX**, was synthesized in accordance with literature procedures.[15] *S*-(1-Methyl-4-hydroxyethyl acetate) *O*-ethyl dithiocarbonate (2.02 g, 8.45 mmol) and pyridine (0.96 mL, 11.83 mmol) were dissolved in dry dichloromethane (DCM, 10 mL). 2-Chloropropionyl chloride (1.18 mL, 11.83 mmol) was diluted in 5 mL of dry DCM and then was gradually added to the solution over 30 min while the solution temperature was kept at around 0 °C. The reaction mixture was stirred for 19 h at room temperature. The excess 2-chloropropionyl chloride was neutralized with 0.1 mL of water and DCM to a total volume of 40 mL. The mixture was poured into a solution of hydrochloric acid (80 mL, 0.3 M). The organic layer was washed with a solution of sodium hydroxide (40 mL, 0.3 M) twice and then dried over $MgSO_4$. The product was purified by flash column chromatography on basic alumina using diethyl ether as eluent, providing 1.136 g (yield = 40.8%) of yellow viscous liquid. ^{1}H NMR ($CDCl_3$, δ = ppm): 4.64 (q, −S═C-OC$H_2$$CH_3$, 2H), 4.47−4.32 (m, −SCSC*H*CH_3, −O(CH_2)$_2$O−, and −OCOC*H*-$ClCH_3$, 6H), 1.83 (d, −OCOCHClCH_3, 3H), 1.58 (d, -SCSCHCH_3, 3H), 1.42 (t, −S═C-OCH_2CH_3, 3H). The ^{1}H NMR spectra of the NVP dimer and two chloroxanthate inifers are shown in the Supporting Information.

Synthesis of *S*-[1-Methyl-4-(6-chloroisobutyrate)Ethyl Acetate] *O*-Ethyl Dithiocarbonate (CiBX). The chloroxanthate inifer **CiBX** was synthesized using halogen exchange.[64−66] A 100 mL Schlenk flask was charged with **BiBX** (1.0 g, 2.58 mmol), bpy (2.42 g, 15.48 mmol), and dry acetone (50 mL), and was then deoxygenated by three freeze−pump−thaw cycles. CuCl (0.511 g, 5.16 mmol) and $CuCl_2$ (0.346 g, 2.58 mmol) were quickly added to the frozen mixture, followed by three freeze−pump−thaw cycles, and the mixture was stirred for 24 h at 50 °C. The mixture was passed through a column filled with neutral alumina to remove the copper. The washing and filtrate solutions were combined and then concentrated to dryness under vacuum to obtain a yellowish liquid in quantitative yield. ^{1}H NMR ($CDCl_3$, δ = ppm): 4.64 (q, −S═C-OC$H_2$$CH_3$, 2H), 4.47−4.32 (m, −SCSC*H*CH_3, and -O(CH_2)$_2$O−, 5H), 1.83 (s, −OCOCH-(CH_3)$_2$, 6H), 1.58 (d, −SCSCHCH_3, 3H), 1.42 (t, −S═C-OCH_2CH_3, 3H).

General Procedure for RAFT Polymerization of NVP. In a typical experiment, **CPX** (16.2 mg, 49×10^{-3} mmol), AIBN (4.1 mg, 25×10^{-3} mmol), anisole (0.26 mL), and NVP (1.05 mL, 9.85 mmol) were charged to a Schlenk flask. The mixture was deoxygenated by three freeze−pump−thaw cycles. The flask was placed in an oil bath thermostatted at 60 °C for the desired time period. Samples were withdrawn at timed intervals via a syringe for the measurement of monomer conversion and molecular weight (MW) of polymer by DMF GPC. The reaction was quenched by placing the flask in an ice bath, exposure to air, and dilution in THF to provide the X-PNVP-ClI macroinitiator. MW of X-PNVP-ClI was measured by GPC, and its xanthate end group was analyzed by ^{1}H NMR (conversion = 18.8%, $M_{n,GPC}$ = 4,500 g/mol, M_w/M_n = 1.15, $M_{n,NMR}$ = 4,550).

General Procedure for ATRP of MMA, MA, and St with CPX or X-PNVP-Cl Macroinitiator. In a typical experiment, X-PNVP-ClI macroinitiator (148 mg, 32×10^{-3} mmol, M_n = 4,500 g/mol, M_w/M_n = 1.15) and anisole (2 mL) were charged to a flask and purged with N_2 for 30 min. Deoxygenated MMA (2 mL, 17.92 mmol), CuCl (4.1 mg, 28×10^{-3} mmol), $CuCl_2$ (0.7 mg, 3.2×10^{-3} mmol), and TPMA (9.3 mg, 32×10^{-3} mmol) were added. An initial sample was taken, and the solution was stirred at 40 °C for the desired time period. At timed intervals, samples were withdrawn via a syringe for measurements of monomer conversion by ^{1}H NMR and MW of polymer by GPC. The polymerization was stopped by placing the flask in an ice bath, exposure to air, and dilution in THF (M_n = 30,700 g/mol, M_w/M_n = 1.20, conversion = 44.2%).

Analyses. ^{1}H NMR spectra were recorded on a Bruker Avance 300 MHz NMR instrument in $CDCl_3$ at 25 °C. Conversions of styrene, (meth)acrylate, and NVP were determined by ^{1}H NMR. MW and molecular weight distribution (M_w/M_n) were measured on a DMF (with PMMA standards) or THF (with PSt standards) GPC system consisting of a Waters 510 HPLC pump, three Waters UltraStyragel columns (10^2, 10^3, and

Scheme 1. Proposed NVP Dimerization Mechanism from Bromoxanthate Inifers

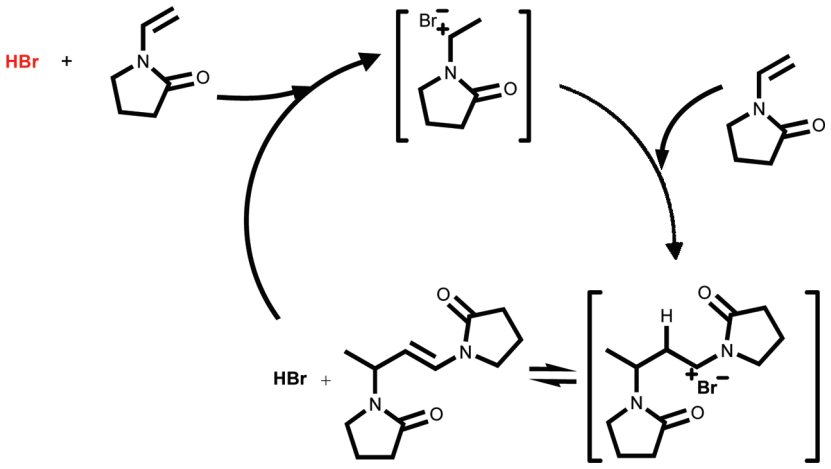

Scheme 2. Synthetic Routes for (a) 2-Chloropropionate Ethyl-2-Xanthate (CPX) by Esterification and (b) 2-Chloroisobutyrate Ethyl-2-Xanthate (CiBX) by Halogen Exchange

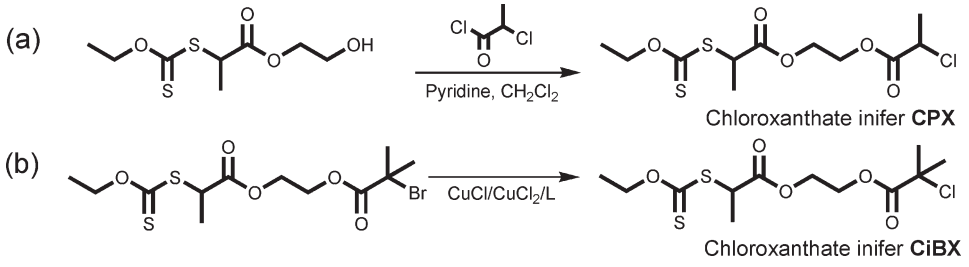

10^5 Å), and a Waters 410 differential refractive index detector, with a flow rate of 1.0 mL/min (30 °C).

Results and Discussion

Model Studies of the *N*-Vinylpyrrolidone (NVP) Dimerization Reaction. The initial attempts to conduct RAFT polymerization of NVP, unexpectedly, led to a nearly quantitative dimerization of NVP in the presence of a small amount bromoxanthate inifers (see Figure S1 in Supporting Information for dimer structure). The acid-catalyzed[63,67–70] and alcohol-catalyzed[63] dimerizations of NVP have been previously reported. The dimerization plausibly proceeds by a cationic mechanism. The S_N2 reaction between the bromoester and a NVP monomer could initiate dimerization. However, the increase of steric hindrance in alkyl bromides from secondary (**BPX**) to tertiary (**BiBX**) (entries S1 and S2 in Table S1, Supporting Information) did not prevent dimerization. Addition of a proton scavenger (DtBuP) resulted in some suppression and retardation of dimer formation (entries S3 (NVP/**BiBX**/AIBN/DtBuP = 200/1/0.5/0.1) and S4 (NVP/**BiBX**/AIBN/DtBuP = 200/1/0.5/2) in Table S1, Supporting Information) but no polymer was detected in DMF GPC traces. Quantitative dimerization of NVP was also observed in the presence of ethyl 2-bromopropionate (EBP) and ethyl 2-bromoisobutyrate (EBiB), analogues of **BPX** and **BiBX**, respectively (Figures S2a and S2b in Supporting Information).

As proposed in Scheme 1, the bromoester-catalyzed dimerization of NVP could proceed via protonation of NVP with traces of HBr and dimer formation with another NVP unit, followed by release of HBr to start a new dimerization cycle.

The NVP dimerization was suppressed by decreasing the electrophilicity of the haloester group. Indeed, no NVP dimer was observed with either a secondary or a tertiary chloroester (ECP or ECiB). The vinyl protons from NVP remained unchanged, and no dimer (no peak at around 4.85 ppm in the ^{1}H NMR spectra) was detected even after 54 h of reaction, as shown in Figures S2c and S2d in Supporting Information. Hence, the dimerization reaction strongly depends on the structure of the haloesters ($Br^- \gg Cl^-$). The absence of the formation of NVP dimer with chloroesters suggests that difunctional chloroxanthate inifers could be used for the preparation of well-defined PNVP block copolymers.

Synthesis of Chloroxanthate Inifers. As shown in Scheme 2, two synthetic strategies were applied to the synthesis of chloroxanthate inifers suitable for the preparation of PNVP-based block copolymers: (a) esterification of *S*-(1-methyl-4-hydroxyethyl acetate) *O*-ethyl dithiocarbonate to form a chloroxanthate inifer with a secondary chloroester moiety and (b) halogen exchange using **BiBX** to form a chloroxanthate inifer with a tertiary chloroester moiety.

2-Chloropropionate ethyl-2-xanthate (**CPX**) (Figure S3, Supporting Information) was prepared by esterification of 2-hydroxyethyl 2-xanthate using a procedure similar to that used for the preparation of bromoxanthate inifers.[15] However, 2-chloroisobutyryl chloride, needed for 2-chloroisobutyrate ethyl-2-xanthate (**CiBX**), is not commercially available. Therefore, following previous reports,[64–66] halogen exchange was used to prepare **CiBX** from the bromoderivative. As shown in Figure S4 (Supporting Information), the chemical shift of $-CH_3$ groups next to the halogen shifted significantly upfield from 1.93 ppm to 1.77 ppm. Table S2 (Supporting Information) summarizes the reaction conditions and results. High purity **CiBX** was obtained using the $CuCl/CuCl_2$/bpy for the halogen exchange. Thus, **CiBX** and **CPX** inifers were successfully synthesized and subsequently evaluated for the controlled polymerization of methyl methacrylate (MMA), styrene (St), and methyl acrylate (MA).

Table 1. Conditions of RAFT Polymerizations of NVP with Chloroxanthate (CX) Inifers[a]

entry	CX	time (h)	conv. (%)	$M_{n,th}$ (g/mol)	$M_{n,GPC}$[b] (g/mol)	M_w/M_n	induction time (h)
1[c]	**CiBX**	24.5	69.4	15,700	17,400	1.40	8.2
2[d]	**CPX**	16.9	56.2	12,800	9,700	1.38	2.9

[a] Performed in 20% (v/v) anisole with a ratio of NVP/CX/AIBN = 200/1/0.5 at 60 °C. [b] M_n was determined by DMF GPC using PMMA calibration. [c] Macroinitiator X-PNVP-ClI ($M_{n,NMR}$ = 4,450, $M_{n,GPC}$ = 4,400, and M_w/M_n = 1.15) was obtained at 19.2% conversion. [d] Macroinitiator X-PNVP-ClII ($M_{n,NMR}$ = 4,550, $M_{n,GPC}$ = 4,500, and M_w/M_n = 1.15) was obtained at 18.8% conversion.

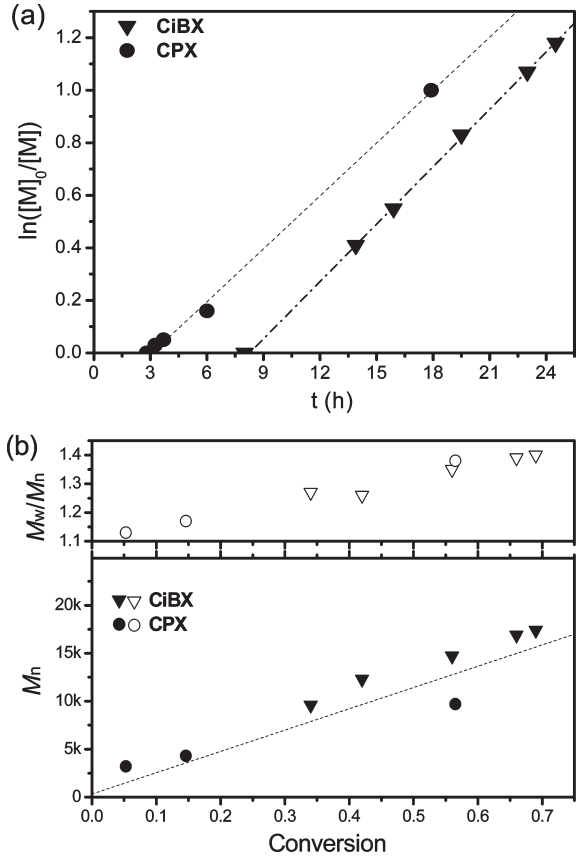

Figure 1. (a) Kinetic plots of monomer conversion vs time and (b) dependence of M_n and M_w/M_n vs conversion in RAFT polymerization of NVP with different chloroxanthate (CX) inifers: NVP/CX/AIBN = 200/1/0.5 in 20% (v/v) anisole at 60 °C.

Preparation of PNVP by RAFT Polymerization. The RAFT polymerization of NVP with the two chloroxanthate inifers was studied. The conditions and results of NVP polymerization are summarized in Table 1. Induction periods of 8 and 3 h were observed with **CiBX** (entry 1) and with **CPX** (entry 2), respectively. Such induction periods were previously reported in RAFT polymerization of less reactive monomers.[71,72] The inhibition may be due to slow fragmentation of the intermediate radicals during the RAFT polymerization. Figure 1a shows linear first-order kinetic plots of NVP obtained with the two different chloroxanthate inifers and shows similar reaction rates after the induction periods. Figure 1b illustrates a linear increase of molecular weight (MW) vs monomer conversion. Polymers with relatively narrow molecular weight distribution (M_w/M_n < 1.4) were obtained. Figure 2 shows monomodal GPC traces, which gradually shift to higher MW. These results indicate well-controlled polymerizations of NVP using the chloroxanthate inifers.

RAFT-First Approach for the Preparation of Block Copolymers. The α,ω-difunctional X-PNVP-Cl polymers were used for the subsequent chain extension with St, MMA, and MA via ATRP.

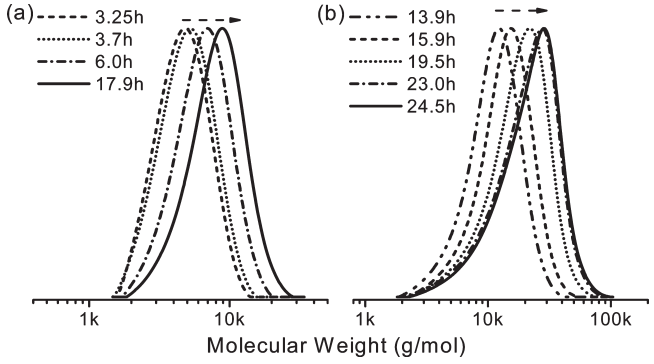

Figure 2. GPC traces of PNVP formed in the presence of chloroxanthate inifers (a) **CiBX** and (b) **CPX**. NVP/CX/AIBN = 200/1/0.5 in 20% (v/v) anisole at 60 °C.

A. Chain Extension of the PNVP Macroinitiator with St. The α,ω-difunctional X-PNVP-Cl was used as an ATRP macroinitiator with chloroester end group to synthesize a PNVP-*b*-PSt block copolymer. Prior to the block copolymerization, St was polymerized with AIBN as the radical source and a monofunctional PNVP-X (see entry S5 in Table S1 in Supporting Information) as the macromolecular chain transfer agent (macroCTA) in order to evaluate the potential chain transfer to the xanthate end group. As shown in Figures 3a and b, the polymerization of St from a monofunctional PNVP-X macroCTA shows a typical behavior of a conventional free radical polymerization (FRP), i.e., no increase of MW with conversion, high MW polymer formed at the beginning of the polymerization (M_n = 37,900 g/mol), and relatively broad molecular weight distribution (M_w/M_n = 1.6−1.8). In Figure 3c, GPC traces of the polymer in DMF clearly showed two distinct populations. The MWs of these two populations do not vary with time and only the relative intensities of the peaks change. The low MW population corresponds to the initial PNVP macroCTA, while the higher MW population corresponds to the PSt homopolymer formed by conventional FRP. In Figure 3d, GPC traces of the polymer in THF showed only a single population of high MW of PSt. The low intensity of PNVP macroCTA in the THF GPC trace is due to the small refractive index differences between PNVP and THF. Despite the weak intensity of PNVP macroCTA, GPC traces in THF also support a conventional FRP of St. These results indicate that PNVP-X is a poor macroCTA in RAFT polymerization of St.

Thus, the α,ω-difunctional X-PNVP-Cl polymers can be used to selectively conduct the chain extension of St by ATRP via catalytic C−Cl bond activation. Since PNVP can chelate metal ions[73,74] and affect the activation/deactivation equilibrium of ATRP, a strong complexing ligand, TPMA,[75] was used for the ATRP of St. Also, a relatively low temperature (60 °C) was selected to minimize potential side reactions (e.g., elimination of the xanthate chain end group).[63] Figures 4a and b shows a linear first-order kinetic plot for the St polymerization and a gradual increase in MW with monomer conversion (St/X-PNVP-ClII/CuCl/$CuCl_2$/TPMA = 770/1/0.975/0.025/1; X-PNVP-ClII, M_n = 4,500

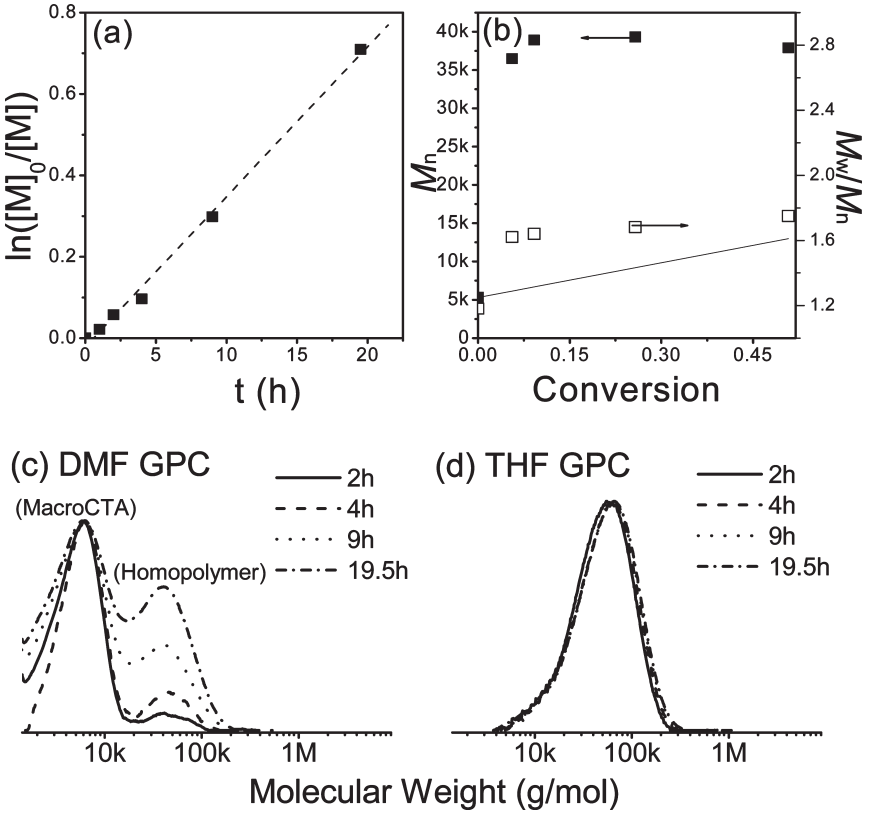

Figure 3. (a) Kinetic plots of monomer conversion vs time, (b) M_n and M_w/M_n vs conversion plots, (c) DMF, and (d) THF GPC traces of St chain extension from PNVP-X macroCTA in 50% (v/v) anisole at 60 °C. St/PNVP-X/AIBN = 145/1/0.1; PNVP-X, M_n = 5,300 and M_w/M_n = 1.21 (entry S5 in Table S1, Supporting Information).

and M_w/M_n = 1.15 (footnote in Table 1)). The experimental molecular weight ($M_{n,GPC}$ = 15,000 g/mol) was lower than the theoretical one ($M_{n,th}$ = 24,400 g/mol for conversion = 24.8%), plausibly because of the difference in hydrodynamic volumes between the block copolymers as well as the use of PMMA standards. The molecular weight determined by ^{1}H NMR ($M_{n,NMR}$ = 19,000 g/mol) provided a value closer to the $M_{n,th}$. The DMF GPC traces present a small tailing toward low MW, which could be due to the presence of some unreacted PNVP macroinitiator. After the block copolymer was purified by precipitation in MeOH, however, no significant decrease in the tailing of the GPC traces was observed (Figure 4c red line). This rules out the presence of unreacted PNVP macroinitiator. The profiles of both DMF (Figure 4c) and THF (Figure 4d) GPC traces as well as narrow molecular weight distributions (M_w/M_n < 1.4) suggest that well-defined PNVP-*b*-PSt block copolymers were obtained.

B. Chain Extension of PNVP Macroinitiator with MMA. MMA was first polymerized with AIBN as the radical source and a monofunctional PNVP-X (see entry S5 in Table S1 in Supporting Information) as macroCTA to evaluate a potential contribution from the RAFT mechanism. As shown in Figure S5 (Supporting Information), a typical conventional FRP polymerization of MMA in the presence of the PNVP-X macroCTA was observed. A polymer with a high molecular weight (M_n = 362,000 g/mol) and a broad molecular weight distribution (M_w/M_n = 2.4) was obtained from the beginning of the polymerization. These results suggest that PNVP-X macroCTA has even lower efficiency as a radical transfer agent for MMA than for St. Hence, the α,ω-difunctional X-PNVP-Cl polymer could be used to selectively conduct the subsequent chain extension with MMA via ATRP.

TPMA was also used as the ligand for chain extension of MMA (MMA/X-PNVP-ClI/CuCl/$CuCl_2$/TPMA = 560/1/0.85/0.15/1; X-PNVP-ClI, M_n = 4,400 and M_w/M_n = 1.15 (footnote in Table 1)). Figures 5a and b shows a linear first-order kinetic plot and a linear increase in MW with monomer conversion during MMA polymerization. The experimental molecular weight ($M_{n,GPC}$ = 50,600 g/mol) was higher than the theoretical one ($M_{n,th}$ = 23,500 g/mol at conversion = 34.1%), plausibly due to the difference in hydrodynamic volumes between the block copolymers. Determination of MW from the ^{1}H NMR spectrum ($M_{n,NMR}$ = 22,500 g/mol) provided a value much closer to the $M_{n,th}$. DMF and THF GPC traces (Figures 5c and d) show monomodal profiles and narrow molecular weight distributions (M_w/M_n < 1.3). These results indicate that well-defined PNVP-*b*-PMMA block copolymers were synthesized.

C. Chain Extension of PNVP Macroinitiator with BA/MA. BA was polymerized under RAFT conditions using AIBN as the radical source and a PNVP-X as macroCTA (see entry S5 in Table S1 in Supporting Information) (BA/PNVP-X/AIBN = 151/1/0.1 in 50% (v/v) anisole at 60 °C) to evaluate chain transfer efficiency of the xanthate moiety of α,ω-difunctional X-PNVP-Cl polymers for acrylates. In contrast to St and MMA polymerization, the MWs increased linearly with conversion and were close to theoretically predicted values, as shown in Figures 6a and b. This indicates that PNVP-X can act as a macroCTA for chain extension of acrylates. GPC traces in THF (Figure 6d) show gradual MW evolution; however, GPC traces in DMF (Figure 6c) show low initiation efficiency and even bimodality with broad molecular weight distributions (M_w/M_n = 1.8−2.4). This reveals that PNVP-X is not a very efficient macroCTA for chain extension with acrylates. Hence, the

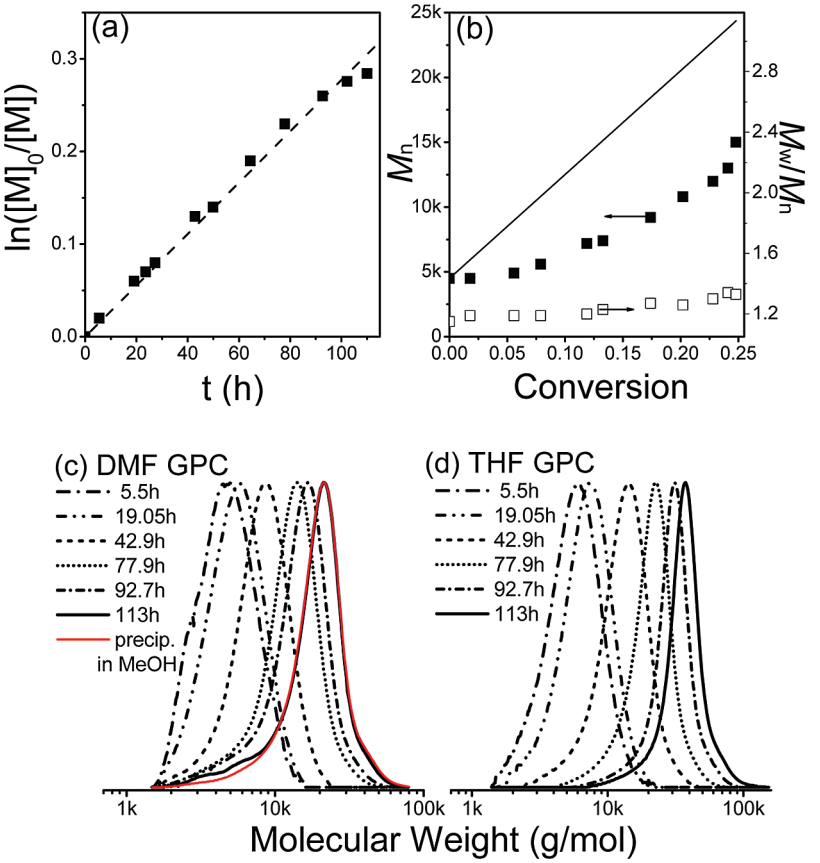

Figure 4. (a) Kinetic plot of monomer conversion vs time, (b) M_n and M_w/M_n vs conversion plots, (c) DMF, and (d) THF GPC traces of St chain extension from X-PNVP-ClII macroinitiator in 50% (v/v) anisole at 60 °C. St/X-PNVP-ClII/CuCl/$CuCl_2$/TPMA = 770/1/0.975/0.025/1; X-PNVP-ClII, M_n = 4,500 and M_w/M_n = 1.15 (footnote in Table 1).

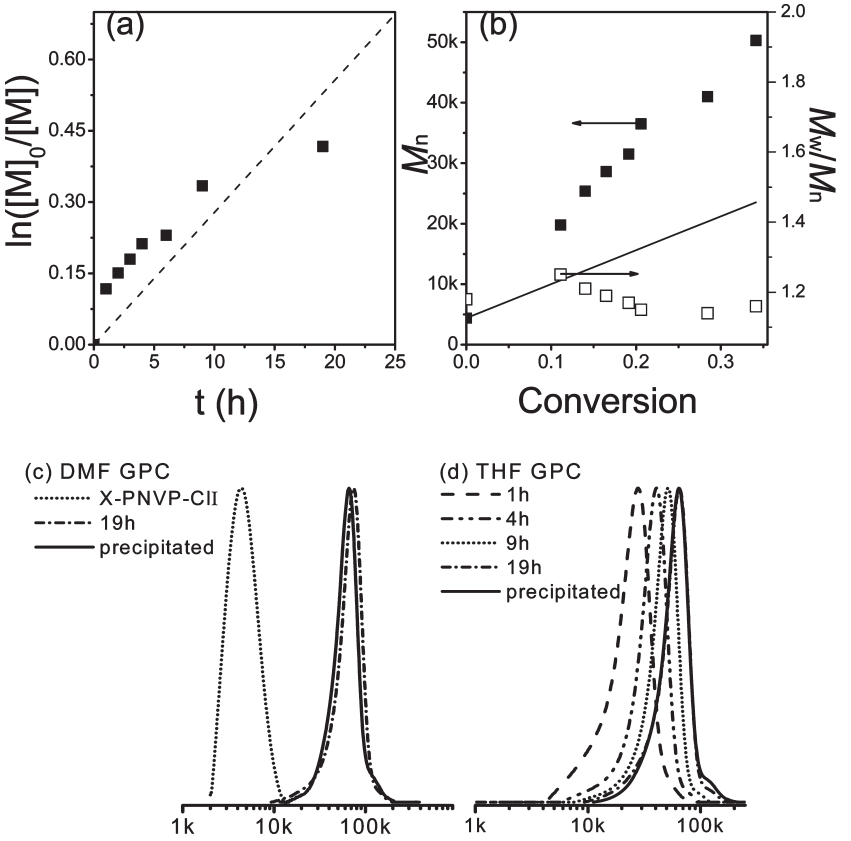

Figure 5. (a) Kinetic plot of monomer conversion vs time, (b) M_n and M_w/M_n vs conversion plots, (c) DMF, and (d) THF GPC traces of MMA chain extension from X-PNVP-ClI macroinitiator in 50% (v/v) anisole at 40 °C. MMA/X-PNVP-ClI/CuCl/$CuCl_2$/TPMA = 560/1/0.85/0.15/1; X-PNVP-ClI, M_n = 4,400 and M_w/M_n = 1.15 (footnote in Table 1).

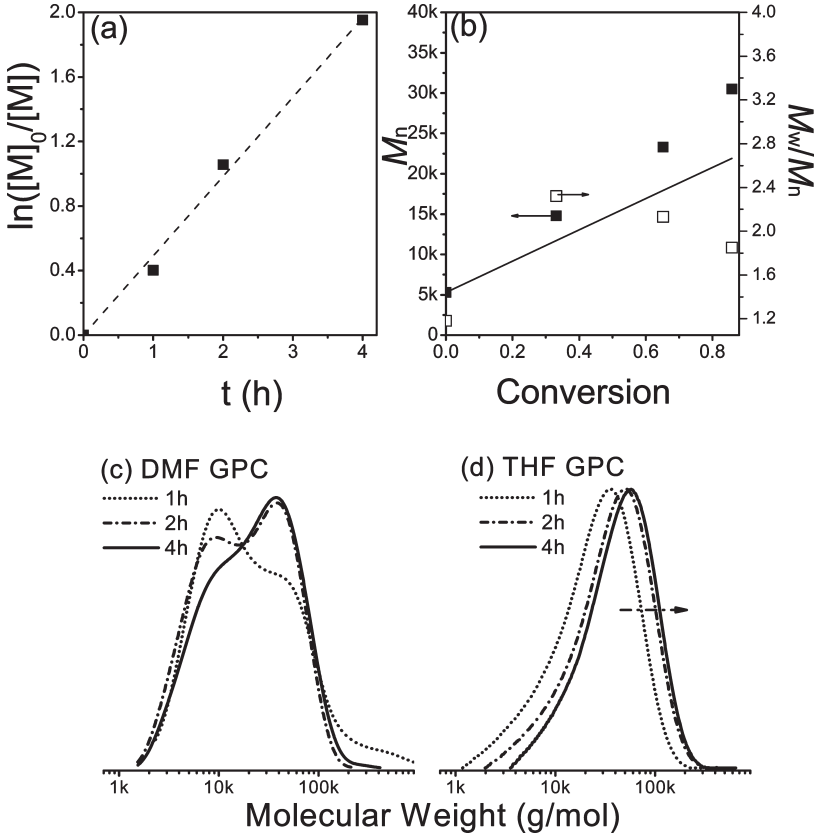

Figure 6. (a) Kinetic plot of monomer conversion vs time, (b) M_n and M_w/M_n vs conversion plots, (c) DMF, and (d) THF GPC traces of BA chain extension from PNVP-X macroCTA in 50% (v/v) anisole at 60 °C. BA/PNVP-X/AIBN = 151/1/0.1; PNVP-X, M_n = 5,300 and M_w/M_n = 1.21 (entry S5 in Table S1, Supporting Information).

Scheme 3. Proposed Chain Transfer to Xanthate during ATRP of MA from PNVP Macroinitiator: Species I and III Can Be ATRP-Active, Species II and IV Are ATRP-Inactive

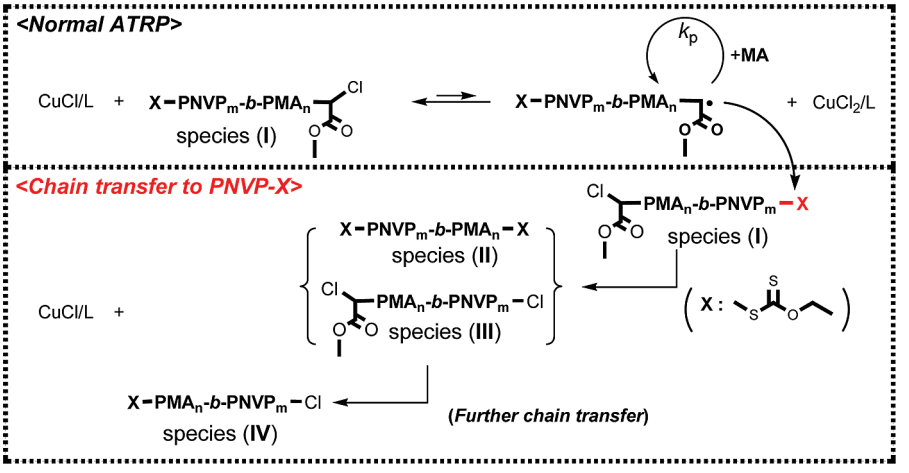

α,ω-difunctional X-PNVP-Cl polymers cannot be used to selectively conduct the subsequent chain extension with BA via ATRP.

To further understand the influence of chain transfer on the chain extension from an α,ω-difunctional X-PNVP-Cl polymer, an ATRP of MA was conducted from the X-PNVP-ClII macroinitiator (footnote in Table 1) (MA/X-PNVP-ClII/CuCl/$CuCl_2$/TPMA = 1000/1/0.9/0.1/1 in 50% (v/v) anisole at 60 °C). As anticipated, chain extension with MA was unsuccessful. Figure 7a shows that the polymerization stopped at very low conversion (3.6% after 70 h). Figures 7b and c show nonlinear molecular weight growth, bimodal molecular weight distributions, and a poor initiation efficiency during the chain extension reaction. A possible explanation for these observations is shown in Scheme 3. When PMA propagating radical transfers to a xanthate moiety (X) during the ATRP, a new species III (**Cl-PMA$_n$-*b*-PNVP$_m$-Cl**) can be formed that can grow to form a PNVP-*b*-PMA diblock copolymer. Concurrently, a double xanthate-ended polymer, species II (**X-PMA$_n$-*b*-PNVP$_m$-X**), which cannot be activated by the copper catalyst, should be generated. As the ATRP progresses, this reshuffling reaction between acrylate propagating radicals and xanthates leads to the formation of species IV (**X-PMA$_n$-*b*-PNVP$_m$-Cl**), and polymerization stops at low conversion.

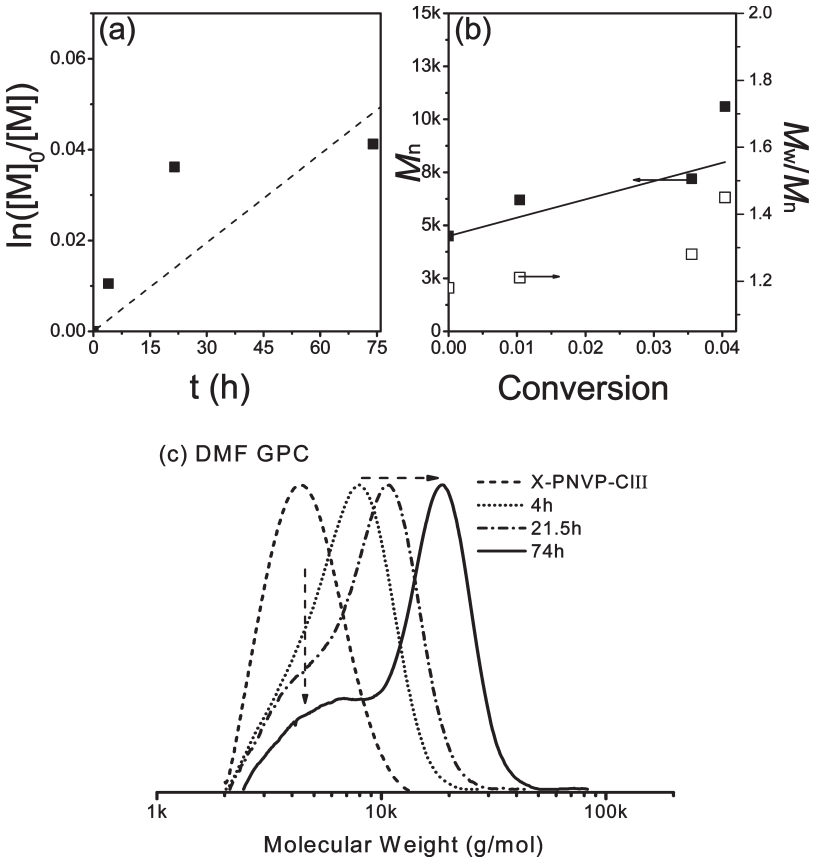

Figure 7. (a) Kinetic plot of monomer conversion vs time, (b) M_n and M_w/M_n vs conversion plots, and (c) DMF GPC traces of MA chain extension from X-PNVP-ClII macroinitiator in 50% (v/v) anisole at 60 °C. MA/X-PNVP-ClII/CuCl/$CuCl_2$/TPMA = 1000/1/0.9/0.1/1; X-PNVP-ClII, M_n = 4,500 and M_w/M_n = 1.15 (footnote in Table 1).

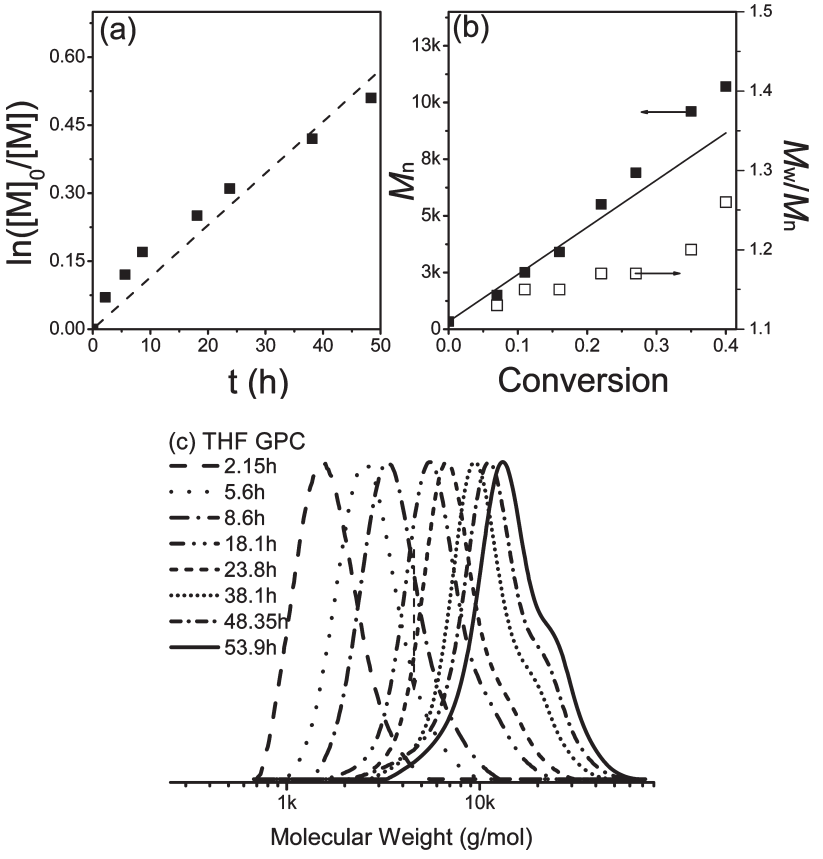

Figure 8. (a) Kinetic plot of monomer conversion vs time, (b) M_n and M_w/M_n vs conversion plots, and (c) THF GPC traces of ATRP of St from **CPX** chloroxanthate inifer in 50% (v/v) anisole at 60 °C. St/**CPX**/CuCl/$CuCl_2$/TPMA = 200/1/0.975/0.025/1.

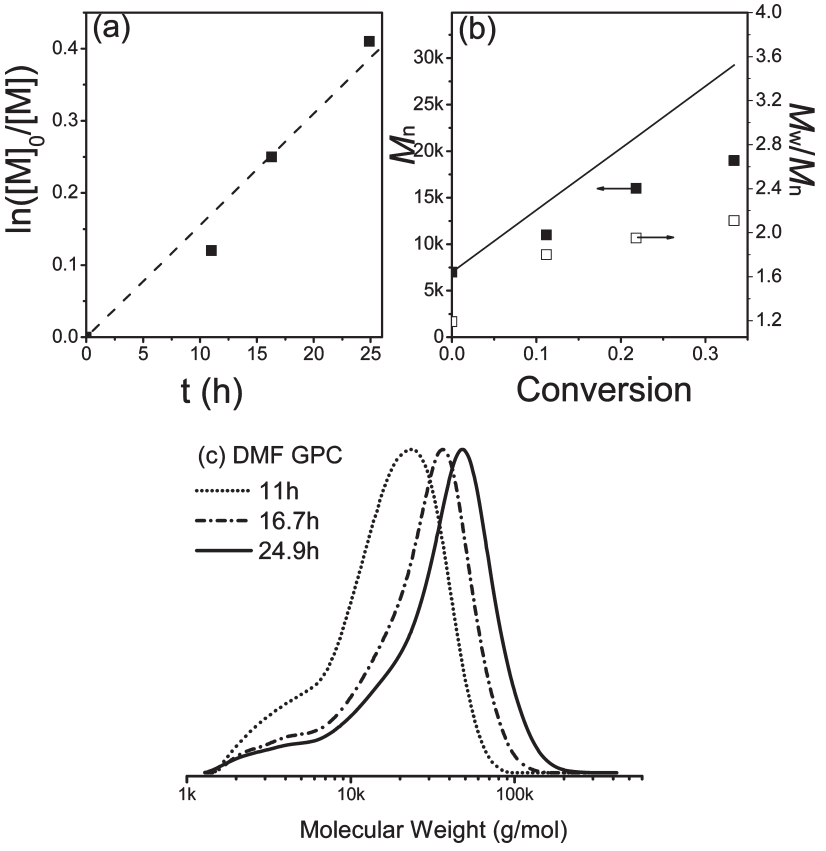

Figure 9. (a) Kinetic plot of monomer conversion vs time, (b) M_n and M_w/M_n vs conversion plots, and (c) DMF GPC traces of NVP chain extension from Cl-PSt-X macroCTA in 40% (v/v) anisole at 60 °C. NVP/Cl-PSt-X/AIBN = 600/1/0.5; Cl-PSt-X, M_n = 7,000 and M_w/M_n = 1.20 (entry S8a in Table S3, Supporting Information).

ATRP-First Approach for the Preparation of Block Copolymers. The alternative polymerization sequence, i.e., using first ATRP of St, MMA, or MA and subsequent RAFT of NVP, was also evaluated for the preparation of PNVP block copolymers. Experimental conditions and the resulting PSt, PMMA, and PMA macroCTAs are summarized in Table S3 in Supporting Information.

A. ATRP of St Followed by RAFT of NVP. Figure 8 shows a kinetic plot of the ATRP of St (St/**CPX**/CuCl/$CuCl_2$/TPMA = 200/1/0.975/0.025/1 in 50% (v/v) anisole at 60 °C). A curvature in the plot of $\ln([M]_0/[M])$ vs time (Figure 8a) indicates that radical concentration decreased during ATRP. MWs increase linearly with conversion, and molecular weight distribution increases above 30% conversion (Figure 8b). A high MW shoulder appeared in the GPC traces after 38 h. The MW of this peak was twice larger than the main PSt peak, and the intensity of the shoulder increased with conversion (Figure 8c). This high MW of the PSt shoulder disappears after hydrolysis of the resulting PSt sample (M_n = 13,000, M_w/M_n = 1.25 (entry S8b in Table S3, Supporting Information)) using sodium hydroxide in THF/methanol (2/1 (v/v)) at 60 °C. No significant change of the population of the main peak was observed (see Figure S6 in Supporting Information). This suggests that the PSt propagating radicals slowly transfer to the xanthate moiety, generating some polymer chains with two propagating species and consequently chains with MWs that were two times higher (cf. Scheme 3). An ester bond in the middle of the higher MW PSt backbone (**Cl-PSt-COO-PSt-Cl**) can be cleaved by hydrolysis, reducing MW. Such a slow chain transfer reaction of the styryl radical to xanthate has been previously reported.[15,62]

A Cl-PSt-X macroCTA (M_n = 7,000, M_w/M_n = 1.20 (entry S8a in Table S3, Supporting Information)) was used for the subsequent RAFT polymerization of NVP (NVP/Cl-PSt-X/AIBN = 600/1/0.5 in 40% (v/v) anisole at 60 °C). Figure 9a shows a first-order kinetic plot for the NVP polymerization; however, a broad molecular weight distribution was observed (Figure 9b). This can be attributed to the existence of some inactive polymer (**Cl-PSt-COO-PSt-Cl**) after the ATRP of St, resulting in a tailing of the GPC curves toward low MW and broadening of the molecular weight distributions (M_w/M_n = 1.9−2.1) (Figure 9c). Thus, first conducting ATRP of St, followed by RAFT of NVP is a less efficient approach for the preparation of PSt-*b*-PNVP block copolymers.

B. ATRP of MMA Followed by RAFT of NVP. A nearly linear relationship between $\ln([M]_0/[M])$ vs time was obtained during the ATRP of MMA with **CiBX** (Figure 10). The controlled nature was further confirmed by a linear increase of MWs with conversion, narrow molecular weight distributions (M_w/M_n < 1.3) of PMMA, and fairly good initiation efficiency ($f = M_{n,th}/M_{n,GPC}$ = 0.8).

Subsequently, a Cl-PMMA-X macroCTA (M_n = 13,000, M_w/M_n = 1.19 (entry S9 in Table S3, Supporting Information)) was used for the subsequent RAFT polymerization of NVP (NVP/Cl-PMMA-X/AIBN = 1000/1/0.5 in 66% (v/v) anisole at 60 °C). Figure 11a shows a first-order kinetic plot for the NVP polymerization, and Figure 11b shows an increase of MWs with conversion and relatively narrow molecular weight distributions (M_w/M_n < 1.3) for monomer conversion lower than 40%. The deviation of MW between $M_{n,th}$ and $M_{n,GPC}$ after 40% monomer conversion might be due to some chain breaking reactions, which can be

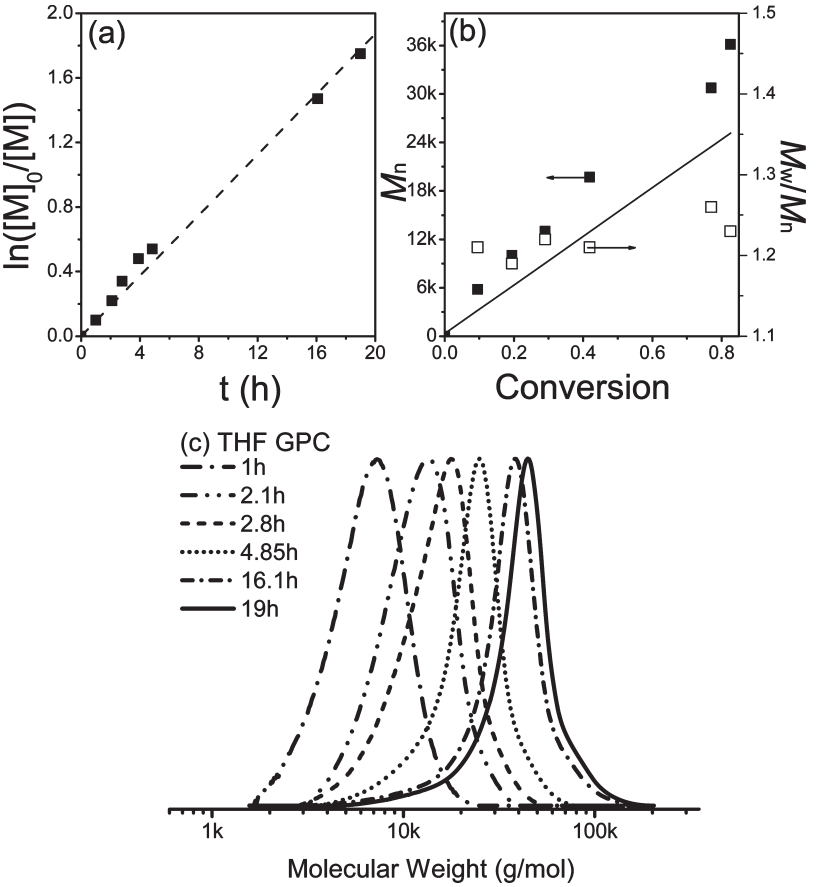

Figure 10. (a) Kinetic plot of monomer conversion vs time, (b) M_n and M_w/M_n vs conversion plots, and (c) THF GPC traces of ATRP of MMA from **CiBX** chloroxanthate inifer in 50% (v/v) anisole at 40 °C. MMA/**CiBX**/CuCl/$CuCl_2$/ PMDETA = 300/1/0.9/0.1/1.

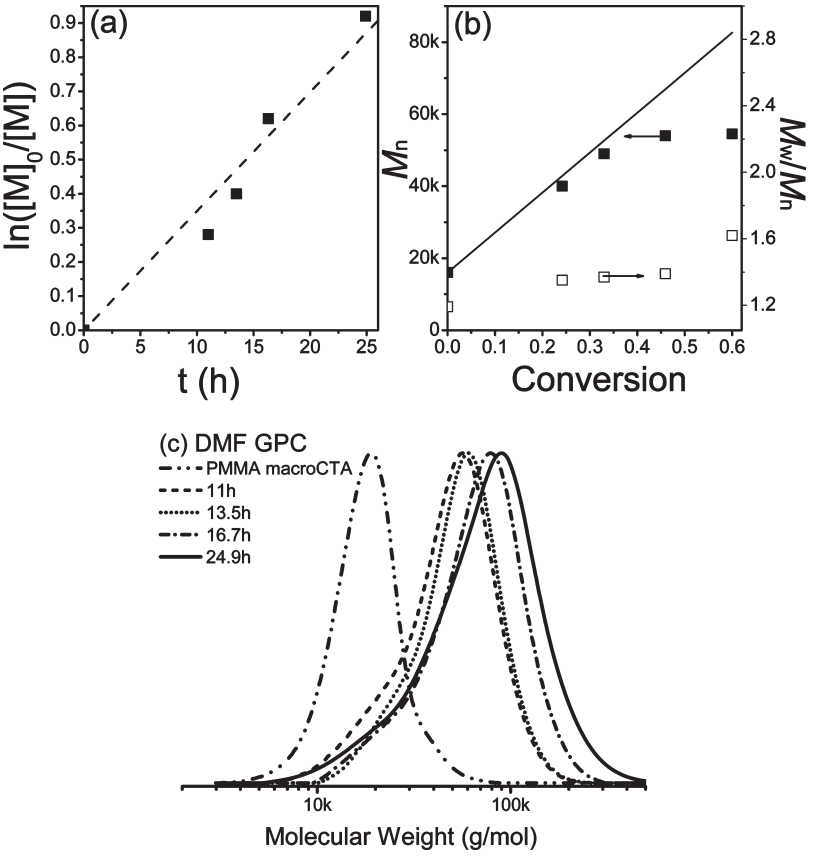

Figure 11. (a) Kinetic plot of monomer conversion vs time, (b) M_n and M_w/M_n vs conversion plots, and (c) DMF GPC traces of NVP chain extension from Cl-PMMA-X macroCTA in 66% (v/v) anisole at 60 °C. NVP/Cl-PMMA-X/AIBN = 1000/1/0.5; Cl-PMMA-X, M_n = 13,000 and M_w/M_n = 1.19 (entry S9 in Table S3, Supporting Information).

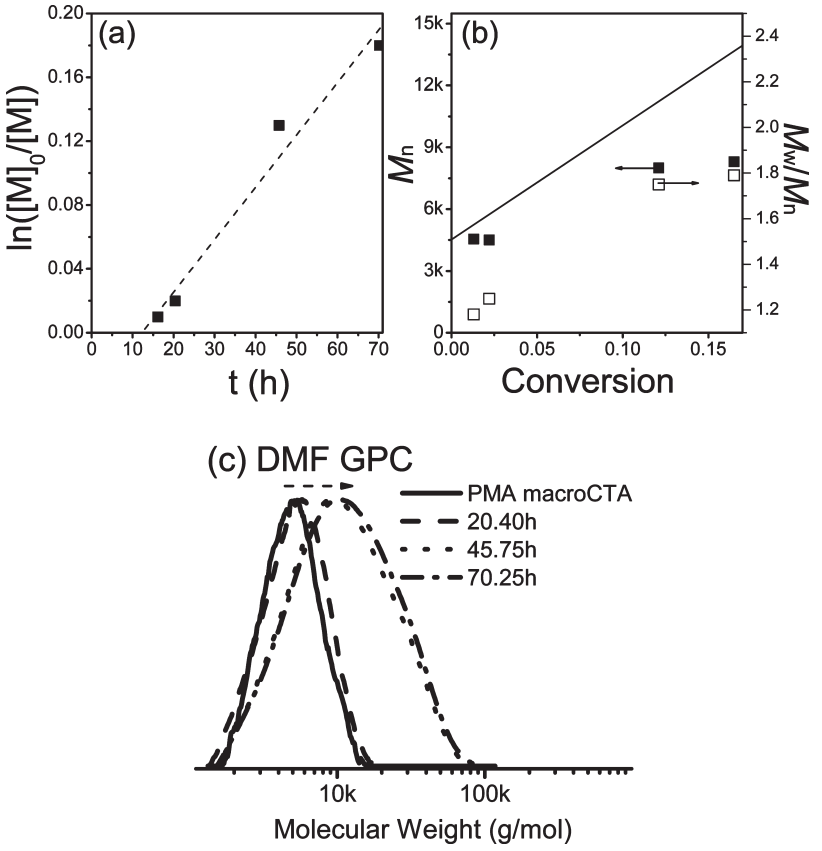

Figure 12. (a) Kinetic plot of monomer conversion vs time, (b) M_n and M_w/M_n vs conversion plots, and (c) DMF GPC traces of NVP chain extension from Cl-PMA-X macroCTA in 50% (v/v) anisole at 60 °C. NVP/Cl-PMA-X/AIBN = 500/1/0.5; Cl-PMA-X, M_n = 3,000 and M_w/M_n = 1.25 (entry S10 in Table S3, Supporting Information).

Scheme 4. Proposed Chain Transfer to the Xanthate Part during ATRP of MA: Difunctional Species I and Species II Were Produced Which Are Both Active for Subsequent RAFT Polymerization

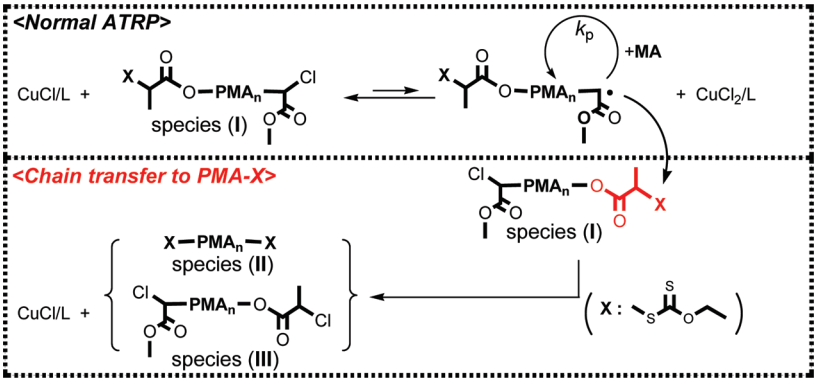

confirmed from a tailing of the GPC curves toward low MW (Figure 11c). These results confirmed the orthogonality between ATRP of MMA and RAFT of NVP using **CiBX** chloroxanthate inifer, at least at lower conversion.

C. ATRP of MA Followed by RAFT of NVP. A Cl-PMA-X macroCTA was prepared in the presence of a chloroxanthate inifer **CPX** with a ratio of MA/**CPX**/CuCl/$CuCl_2$/PMDETA = 200/1/0.8/0.2/1 in 50% (v/v) anisole at 60 °C. A resulting Cl-PMA-X macroCTA (M_n = 4,400 and M_w/M_n = 1.19 (entry S10 in Table S3, Supporting Information)) was used for chain extension of NVP. Figure 12a shows a first-order kinetic plot for NVP polymerization. A limited increase in MW and rather high polydispersities were observed after 45 h in Figures 12b and c. The cause of this poor control over polymerization might arise from the occurrence of chain transfer reactions between acrylate radicals and the xanthate moiety during ATRP of MA. This chain transfer reaction is similar to the above-mentioned case of ATRP of St. A detailed explanation is proposed in Scheme 4 (i.e., an example for ATRP of MA with **CPX**).

Scheme 4 illustrates the proposed formation of three PMA macroCTA species during the ATRP reaction: (a) regular species I (**Cl-PMA-X**), (b) transfer of the propagating radical to a xanthate moiety to form species II (**X-PMA-X**), and (c) species III (**Cl-PMA-Cl**). Species II is inactive during ATRP but could generate a macromolecule with MW that is two times higher during the subsequent RAFT polymerization of NVP. The chain transfer reactions gradually occur, generating species II and III with various MWs during the ATRP of MA. This resulted in the broad molecular weight distributions for the subsequent RAFT chain extension of NVP. In contrast to the RAFT-first approach for preparing

PNVP-*b*-PMA (Scheme 3), no species IV can be formed, and the reaction continues. In summary, well-defined PMA-*b*-PNVP block copolymer could not be prepared using either first RAFT polymerization of NVP followed by ATRP of MA or the opposite sequence. This can be ascribed to the high reactivity of the MA radical toward the xanthate moiety, resulting in reshuffling and statistical distribution of ATRP and RAFT chain ends. For the RAFT-first system, this process leads to the X-PMA-PNVP-Cl system that cannot be activated by a copper catalyst, resulting in limited conversion.

Conclusions

Difunctional haloxanthate inifers were used to prepare block copolymers by sequential ATRP of conjugated monomers and RAFT polymerization of NVP. The quantitative dimerization of NVP that occurred in the presence of bromoxanthate inifers was overcome by using two difunctional chloroxanthate inifers (**CPX** and **CiBX**). Well-controlled polymerizations with some induction periods were observed for the RAFT polymerization of NVP. In the subsequent ATRP chain extensions, PNVP-*b*-PSt and PNVP-*b*-PMMA were successfully synthesized, with monomodal GPC profiles and relatively narrow molecular weight distributions. In the case of chain extension with MA a reshuffling reaction between acrylate propagating radicals and xanthate moiety occurred, resulting in the formations of **X-PMA$_n$-*b*-PNVP$_m$-X** and **X-PMA$_n$-*b*-PNVP$_m$-Cl** species, which cannot be activated by the copper catalyst. This results in poor control during the chain extension with MA. When employing the ATRP-first sequence, a well-controlled polymerization was observed only for the ATRP of MMA with the **CiBX** initiator. Some reshuffling reactions between the xanthate moiety and the styryl/acrylate propagating radicals were observed with the **CPX** initiator. This process resulted in the formations of **X-PMA-X** and **Cl-PMA-Cl**, which are active and inactive macroCTAs for the subsequent RAFT polymerization of NVP, respectively. As a result, poor controls and broad molecular weight distributions were observed during the chain extension of NVP from PSt and PMA macroCTAs.

In summary, chloroxanthate inifers provide access to well-defined PNVP-*b*-PMMA and PNVP-*b*-PSt block copolymers, but not to the PNVP-*b*-PMA block copolymer.

Acknowledgment. We thank the NSF (CHE-07-15494 and DMR-0549353) and the members of the CRP Consortium at Carnegie Mellon University for their financial support. C.-F.H. acknowledges the National Science Council and National Chiao Tung University (NSC-096-2120-M-009-009 and NSC-096-2917-I-564-131) for the postdoctoral fellowship. R.N. thanks Dr. and Mrs. McWilliams (Astrid and Bruce McWilliams Fellowship) for their financial support.

Supporting Information Available: ^{1}H NMR spectra, conditions, and results of dimerization, chloroxanthate synthesis, and polymerizations. This material is available free of charge via the Internet at http://pubs.acs.org.

References and Notes

(1) Braunecker, W. A.; Matyjaszewski, K. *Prog. Polym. Sci.* **2007**, *32*, 93–146.
(2) Matyjaszewski, K. In *Controlled/Living Radical Polymerization: Progress in ATRP* Matyjaszewski, K.; Ed.; ACS Symposium Series; American Chemical Society: Washington, DC, **2009**; Vol. *1023*, pp 3−14.
(3) Wang, J. S.; Matyjaszewski, K. *J. Am. Chem. Soc.* **1995**, *117*, 5614–5615.
(4) Matyjaszewski, K.; Xia, J. H. *Chem. Rev.* **2001**, *101*, 2921–2990.
(5) Matyjaszewski, K.; Tsarevsky, N. V. *Nat. Chem.* **2009**, *1*, 276–288.
(6) Tsarevsky, N. V.; Matyjaszewski, K. *Chem. Rev.* **2007**, *107*, 2270–2299.
(7) Gaynor, S. G.; Wang, J. S.; Matyjaszewski, K. *Macromolecules* **1995**, *28*, 8051–8056.
(8) Chiefari, J.; Chong, Y. K.; Ercole, F.; Krstina, J.; Jeffery, J.; Le, T. P. T.; Mayadunne, R. T. A.; Meijs, G. F.; Moad, C. L.; Moad, G.; Rizzardo, E.; Thang, S. H. *Macromolecules* **1998**, *31*, 5559–5562.
(9) Lowe, A. B.; McCormick, C. L. *Prog. Polym. Sci.* **2007**, *32*, 283–351.
(10) Yamago, S.; Kayahara, E.; Kotani, M.; Ray, B.; Kwak, Y.; Goto, A.; Fukuda, T. *Angew. Chem., Int. Ed.* **2007**, *46*, 1304–1306.
(11) Moad, G.; Rizzardo, E.; Thang, S. H. *Polymer* **2008**, *49*, 1079–1131.
(12) Kwak, Y.; Matyjaszewski, K. *Macromolecules* **2008**, *41*, 6627–6635.
(13) Kwak, Y.; Nicolay, R.; Matyjaszewski, K. *Macromolecules* **2008**, *41*, 6602–6604.
(14) Nicolay, R.; Kwak, Y.; Matyjaszewski, K. *Macromolecules* **2008**, *41*, 4585–4596.
(15) Nicolay, R.; Kwak, Y.; Matyjaszewski, K. *Chem. Commun.* **2008**, 5336–5338.
(16) Matyjaszewski, K.; Miller, P. J.; Shukla, N.; Immaraporn, B.; Gelman, A.; Luokala, B. B.; Siclovan, T. M.; Kickelbick, G.; Vallant, T.; Hoffmann, H.; Pakula, T. *Macromolecules* **1999**, *32*, 8716–8724.
(17) Matyjaszewski, K.; Ziegler, M. J.; Arehart, S. V.; Greszta, D.; Pakula, T. *J. Phys. Org. Chem.* **2000**, *13*, 775–786.
(18) Coessens, V.; Pintauer, T.; Matyjaszewski, K. *Prog. Polym. Sci.* **2001**, *26*, 337–377.
(19) Davis, K. A.; Matyjaszewski, K. *Adv. Polym. Sci.* **2002**, *159*, 1–169.
(20) Matyjaszewski, K. *Polym. Int.* **2003**, *52*, 1559–1565.
(21) Oh, J. K.; Drumright, R.; Siegwart, D. J.; Matyjaszewski, K. *Prog. Polym. Sci.* **2008**, *33*, 448–477.
(22) Sheiko, S. S.; Sumerlin, B. S.; Matyjaszewski, K. *Prog. Polym. Sci.* **2008**, *33*, 759–785.
(23) Gao, H. F.; Matyjaszewski, K. *Prog. Polym. Sci.* **2009**, *34*, 317–350.
(24) Matyjaszewski, K.; Patten, T. E.; Xia, J. H. *J. Am. Chem. Soc.* **1997**, *119*, 674–680.
(25) Matyjaszewski, K. *Chem.—Eur. J.* **1999**, *5*, 3095–3102.
(26) Teodorescu, M.; Matyjaszewski, K. *Macromolecules* **1999**, *32*, 4826–4831.
(27) Matyjaszewski, K.; Jo, S. M.; Paik, H. J.; Shipp, D. A. *Macromolecules* **1999**, *32*, 6431–6438.
(28) Jakubowski, W.; Matyjaszewski, K. *Angew. Chem., Int. Ed.* **2006**, *45*, 4482–4486.
(29) Jakubowski, W.; Min, K.; Matyjaszewski, K. *Macromolecules* **2006**, *39*, 39–45.
(30) Pintauer, T.; Matyjaszewski, K. *Chem. Soc. Rev.* **2008**, *37*, 1087–1097.
(31) Xia, J. H.; Paik, H. J.; Matyjaszewski, K. *Macromolecules* **1999**, *32*, 8310–8314.
(32) Wakioka, M.; Baek, K. Y.; Ando, T.; Kamigaito, M.; Sawamoto, M. *Macromolecules* **2002**, *35*, 330–333.
(33) Tang, H. D.; Radosz, M.; Shen, Y. Q. *AIChE J.* **2009**, *55*, 737–746.
(34) Lu, X. J.; Gong, S. L.; Meng, L. Z.; Li, C.; Yang, S.; Zhang, L. F. *Polymer* **2007**, *48*, 2835–2842.
(35) Brar, A. S.; Kaur, S. *J. Polym. Sci., Part A: Polym. Chem.* **2006**, *44*, 1745–1757.
(36) Debuigne, A.; Poli, R.; Jerome, C.; Jerome, R.; Detrembleur, C. *Prog. Polym. Sci.* **2009**, *34*, 211–239.
(37) Li, S.; de Bruin, B.; Peng, C. H.; Fryd, M.; Wayland, B. B. *J. Am. Chem. Soc.* **2008**, *130*, 13373–13381.
(38) Maria, S.; Kaneyoshi, H.; Matyjaszewski, K.; Poli, R. *Chem.—Eur. J.* **2007**, *13*, 2480–2492.
(39) Iovu, M. C.; Matyjaszewski, K. *Macromolecules* **2003**, *36*, 9346–9354.
(40) Yusa, S.; Yamago, S.; Sugahara, M.; Morikawa, S.; Yamamoto, T.; Morishima, Y. *Macromolecules* **2007**, *40*, 5907–5915.
(41) Yamago, S.; Ray, B.; Iida, K.; Yoshida, J.; Tada, T.; Yoshizawa, K.; Kwak, Y.; Goto, A.; Fukuda, T. *J. Am. Chem. Soc.* **2004**, *126*, 13908–13909.
(42) Ray, B.; Kotani, M.; Yamago, S. *Macromolecules* **2006**, *39*, 5259–5265.
(43) Charmot, D.; Corpart, P.; Adam, H.; Zard, S. Z.; Biadatti, T.; Bouhadir, G. *Macromol. Symp.* **2000**, *150*, 23–32.
(44) Stenzel, M. H.; Cummins, L.; Roberts, G. E.; Davis, T. P.; Vana, P.; Barner-Kowollik, C. *Macromol. Chem. Phys.* **2003**, *204*, 1160–1168.

(45) Moad, G.; Rizzardo, E.; Thang, S. H. *Aust. J. Chem.* **2005**, *58*, 379–410.
(46) Benaglia, M.; Chiefari, J.; Chong, Y. K.; Moad, G.; Rizzardo, E.; Thang, S. H. *J. Am. Chem. Soc.* **2009**, *131*, 6914–6915.
(47) Bian, C. R.; Suzuki, S.; Asakura, K.; Ping, L.; Toshima, N. *J. Phys. Chem. B* **2002**, *106*, 8587–8598.
(48) Einaga, H.; Harada, M. *Langmuir* **2005**, *21*, 2578–2584.
(49) Wan, D. C.; Satoh, K.; Kamigaito, M.; Okamoto, Y. *Macromolecules* **2005**, *38*, 10397–10405.
(50) Devasia, R.; Bindu, R. L.; Borsali, R.; Mougin, N.; Gnanou, Y. *Macromol. Symp.* **2005**, *229*, 8–17.
(51) Nguyen, T. L. U.; Eagles, K.; Davis, T. P.; Barner-Kowollik, C.; Stenzel, M. H. *J. Polym. Sci., Part A: Polym. Chem.* **2006**, *44*, 4372–4383.
(52) Hussain, H.; Tan, B. H.; Gudipati, C. S.; Liu, Y.; He, C. B.; Davis, T. P. *J. Polym. Sci., Part A: Polym. Chem.* **2008**, *46*, 5604–5615.
(53) Bilalis, P.; Pitsikalis, M.; Hadjichristidis, N. *J. Polym. Sci., Part A: Polym. Chem.* **2006**, *44*, 659–665.
(54) Bilalis, P.; Zorba, G.; Pitsikalis, M.; Hadjichristidis, N. *J. Polym. Sci., Part A: Polym. Chem.* **2006**, *44*, 5719–5728.
(55) Debuigne, A.; Willet, N.; Jerome, R.; Detrembleur, C. *Macromolecules* **2007**, *40*, 7111–7118.
(56) Luo, L. B.; Ranger, M.; Lessard, D. G.; Le Garrec, D.; Gori, S.; Leroux, J. C.; Rimmer, S.; Smith, D. *Macromolecules* **2004**, *37*, 4008–4013.
(57) Pound, G.; Aguesse, F.; McLeary, J. B.; Lange, R. F. M.; Klumperman, B. *Macromolecules* **2007**, *40*, 8861–8871.
(58) Lee, H. F.; Kuo, S. W.; Huang, C. F.; Lu, J. S.; Chan, S. C.; Wang, C. F.; Chang, F. C. *Macromolecules* **2006**, *39*, 5458–5465.
(59) Matyjaszewski, K.; Beers, K. L.; Kern, A.; Gaynor, S. G. *J. Polym. Sci., Part A: Polym. Chem.* **1998**, *36*, 823–830.
(60) (a) Yagci, Y.; Tasdelen, M. A. *Prog. Polym. Sci.* **2006**, *31*, 1133–1170. (b) Bernaerts, K. V.; Du Prez, F. E. *Prog. Polym. Sci.* **2006**, *31*, 671–722.
(61) (a) Coca, S.; Matyjaszewski, K. *Macromolecules* **1997**, *30*, 2808–2810. (b) Coca, S.; Paik, H.-j.; Matyjaszewski, K. *Macromolecules* **1997**, *30*, 6513–6516. (c) Kajiwara, A.; Matyjaszewski, K. *Macromolecules* **1998**, *31*, 3489–3493. (d) Gaynor, S. G.; Matyjaszewski, K. *Macromolecules* **1997**, *30*, 4241–4243. (e) Shinoda, H.; Matyjaszewski, K. *Macromolecules* **2001**, *34*, 6243–6248. (f) Shinoda, H.; Miller, P. J.; Matyjaszewski, K. *Macromolecules* **2001**, *34*, 3186–3194. (g) Davis, K. A.; Charleux, B.; Matyjaszewski, K. *J. Polym. Sci., Part A: Polym. Chem.* **2000**, *38*, 2274–2283.
(62) Tong, Y. Y.; Dong, Y. Q.; Du, F. S.; Li, Z. C. *Macromolecules* **2008**, *41*, 7339–7346.
(63) Pound, G.; Eksteen, Z.; Pfukwa, R.; McKenzie, J. M.; Lange, R. F. M.; Klumperman, B. *J. Polym. Sci., Part A: Polym. Chem.* **2008**, *46*, 6575–6593.
(64) Matyjaszewski, K.; Shipp, D. A.; Wang, J. L.; Grimaud, T.; Patten, T. E. *Macromolecules* **1998**, *31*, 6836–6840.
(65) Matyjaszewski, K.; Wang, J. L.; Grimaud, T.; Shipp, D. A. *Macromolecules* **1998**, *31*, 1527–1534.
(66) Shipp, D. A.; Wang, J. L.; Matyjaszewski, K. *Macromolecules* **1998**, *31*, 8005–8008.
(67) Breitenbach, J. W. *J. Polym. Sci.* **1957**, *23*, 949–953.
(68) Kaupp, G.; Matthies, D. *Chem. Ber./Recl.* **1987**, *120*, 1897–1903.
(69) Zhuo, J. C. *Molecules* **1999**, *4*, M117–M117.
(70) Madl, A.; Spange, S. *Macromolecules* **2000**, *33*, 5325–5335.
(71) Schilli, C.; Lanzendorfer, M. G.; Muller, A. H. E. *Macromolecules* **2002**, *35*, 6819–6827.
(72) McLeary, J. B.; McKenzie, J. M.; Tonge, M. P.; Sanderson, R. D.; Klumperman, B. *Chem. Commun.* **2004**, 1950–1951.
(73) Caykara, T.; Inam, R.; Ozturk, Z.; Guven, O. *Colloid Polym. Sci.* **2004**, *282*, 1282–1285.
(74) Sun, Y. G.; Xia, Y. N. *Science* **2002**, *298*, 2176–2179.
(75) Xia, J. H.; Matyjaszewski, K. *Macromolecules* **1999**, *32*, 2434–2437.